

Numerical Calculation of Static Strength Performance of Planar Gate Structures

ABSTRACT

As an important part of the ecological environment, rivers provide an important guarantee for the production and life in China. At present, domestic and foreign for the construction of the gate has been gradually shaped, hydraulic steel gate gradually developed as a hydroelectric power station high head, flood discharge flow of large gate type, the smooth opening and closing of the gate is related to the entire water conservancy hub and downstream of the safety of the residents' lives. For the safety of plane gate, this paper adopts Ansys software to establish a finite element model of plane gate, and calculates the most dangerous point stress of plane gate by considering its most unfavourable loading condition. At the same time, the service life of the allowable stress reduction was considered. The analysis results show that the planar gate meets the strength safety. The main beam is simplified into slender beam and thin-walled deep beam, and the calculation formula of slender beam in the mechanics of materials and thin-walled deep beam in the literature is used to calculate the positive bending stress in the mid-span cross-section of the main beam of the gate, and a comparative analysis is carried out with the results of Ansys, which shows that the positive bending stress in the mid-span cross-section of the main beam obtained by simplifying the main beam into a thin-walled deep beam is more close to the results of Ansys calculation. The results of this paper provide an important reference for the structural strength analysis of planar gates.

Keywords: Planar gate; Modal analysis; Strength analysis; Finite element.

1. INTRODUCTION

The metal steel structure of water conservancy project is mainly divided into gate, opener, pressure pipe and cleaner, among which the gate plays an important role in hydropower station as controlling water flow [1]. As shown in Figure 1, the three gates correspond to different degrees of opening, the rightmost gate has been closed, and the left two gates are open. The current required water flow has been coped with. By lifting the height of the gates, the water flow size can be controlled. However, when the gate opens and closes, due to the impact of the water flow, it will inevitably produce vibration. When the frequency of water flow vibration is close to the intrinsic frequency of the gate itself, resonance phenomenon will occur, and then the gate is prone to violent vibration, which will cause damage [2]. Therefore, the research on gate vibration has become the main research direction of current water conservancy workers.

Due to the complexity of the gate structure, the specific theoretical aspects of the calculation is very little. The main reasons for gate failure at home and abroad are broadly divided into two categories [3]: the first category is that the gate itself has insufficient structural strength and corrosion damage occurs. Due to the long service life of the gate, corrosion will inevitably occur. The metal structure of the gate is thinned due to the corrosion of the water, which can not withstand the water pressure and deformation damage occurs [4]; the second category is the vibration damage of the gate. Due to the role of water flow, the gate will occur power instability phenomenon, resulting in the frequency of the water impact gate

close to the gate's own intrinsic frequency, in this case the resonance phenomenon will occur, resulting in a reduction in the gate's own strength[5].



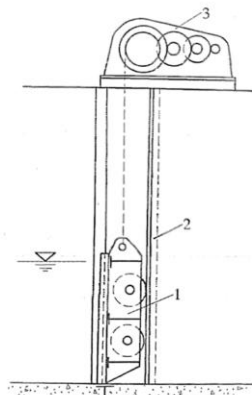
Fig. 1 Flat steel gates application in practical engineering

The design of the current gates is mainly based on the methods in the Design Code for Steel Gates for Water Conservancy and Hydroelectric Engineering [6]. The calculation method of the code is mainly based on the strength analysis for bending stress in the mechanics of materials. For example, the design of the main beam is regarded as a simply supported beam subjected to uniform load. But in fact, the structure of the gate is not a simple simply supported beam, but a complex spatial structure consisting of the main beam, longitudinal partitions and fascia plates. So when designing the gate according to the specification, it will be relatively conservative a lot.

At the same time, with the development of CAE software, the finite element method has also been widely used and developed in water conservancy engineering. At present, the finite element analysis of the gate has become mature, but because the main reason for many gate failures is the vibration that occurs to cause structural damage to the gate as a whole, so there are still a lot of problems that need to be solved for gate vibration [7]. Because the gate itself is a relatively complex structure, coupled with the complexity of the water flow conditions involved, there is still no mature theory can be used to solve this problem, so for the solution of the gate due to the occurrence of vibration and thus damage to the need for more in-depth research.

2. COMPOSITION AND WORKING PRINCIPLE OF THE GATE

The overall structure of the plane gate in this study is shown in Figure 2, which is mainly divided into three parts: fixed embedded parts, opening and closing equipment and door leaf structure. In water conservancy projects, the gate in the fixed embedded parts through the opening and closing equipment (starter, etc.) operation, so that the gate displacement.



1-door leaf; 2-embedded part; 3-opening and closing equipment
Fig. 2 Composition of a plane gate

The gate structure is relatively complex, the orifice on the hydropower station by the gate to open and close, according to the actual production and life needs to adjust. The different heights at which the gates are opened are called openings, and the water pressure on the gates under different openings is also different. The opening and closing of the gates make the upstream water level rise and fall reasonably to achieve the practical significance of the project, such as regulating the flow rate, irrigation, drinking water, power generation, navigation, and discharging of sediment, etc. Therefore, the gate design has a profound influence on the safety of the entire hydraulic hub as well as the lives of people downstream.

Therefore, the gate design has far-reaching influence on the whole water conservancy hub and the safety of people's lives and properties downstream.

Gate groove embedded parts are mainly to bear the conductive door leaf water pressure to the building, and constraints, positioning gate operation, and gate with the completion of the water seal. Plane gate door slot as shown in Figure 3, mainly by the main rail, counter rail, bottom threshold and other components.

The main rail is facing the water flow above the door groove embedded parts, is to bear the main pressure of the gate embedded parts, its side both the gate lateral guide support running tread. Positive water stop gate water seal stop pad is generally arranged in the main track, and gate water seal with the completion of lateral water stop function.

Counter rail is the back to the water flow above the door groove embedded parts, mainly for the gate to play a guiding role, and its side of the gate lateral guided support of the running tread. The gate water seal stopping plate for reverse water stopping is generally arranged on the counter rail, and the gate water seal cooperates with the gate to complete the lateral water stopping function.

The bottom sill mainly bears the vertical pressure of the gate, and its working pedal and the gate bottom water seal cooperate to complete the gate bottom water seal function.



Fig. 3 Door groove embedding

The opening and closing equipment mainly adopts fixed winch type opener. As shown in Figure 4, its composition consists of frame, wire rope, reel and transmission device. The transmission device is divided into brake, reducer, governor and so on. Fixed winch type opener is used in a wide range of scenarios, opening the gate is mainly by overcoming the self-weight of the gate and the friction force. Close the gate is to rely on the self-weight of the gate and the total water pressure to complete the closure of the gate, the same closure of the gate is also required to overcome the gate main track and the contra-rail on the frictional resistance. The working principle of the fixed winch type opener is that the motor drives the open gear and drum through the coupling and reducer with brake, so that the wire rope is wound on the drum, and the opening and closing of the gate is completed through the lifting and releasing of the wire rope.

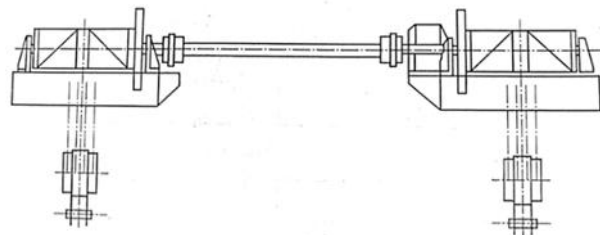


Fig.4 Centrally driven, double-point fixed hoist

The door leaf structure is shown in Fig. 5, which is modelled in equal scale using solidworks software based on the construction drawings. The structure usually consists of panels, edge beams, main beams, longitudinal partitions, secondary beams and so on. The panel is made of Q345 carbon structural steel, the side beams, main beams and lattice beams are usually made of Q345 carbon structural steel, and the cross-section type is usually I-beam or T-beam, and the secondary beams are usually made of channel steel or I-beam.

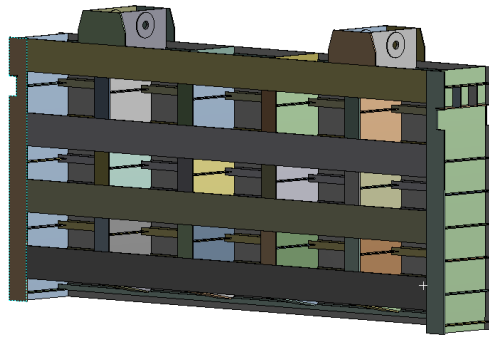


Fig.5 Flat gate model drawing

3.NUMERICAL CALCULATION AND ANALYSIS OF STATIC PERFORMANCE OF PLANE GATE STRUCTURE

3.1FINITE ELEMENT MODEL ESTABLISHMENT OF PLANE GATE

The model was imported into Ansys, and Solid cells were used for meshing in order to calculate the accuracy, and the finite element model was shown in Fig. 6, and the number of cells reached 82602. The modulus of elasticity $E=2.06 \times 10^5 \text{MPa}$, Poisson's ratio $\lambda=0.3$, and the material density $\rho=7.85 \times 10^3 \text{kg/m}^3$.

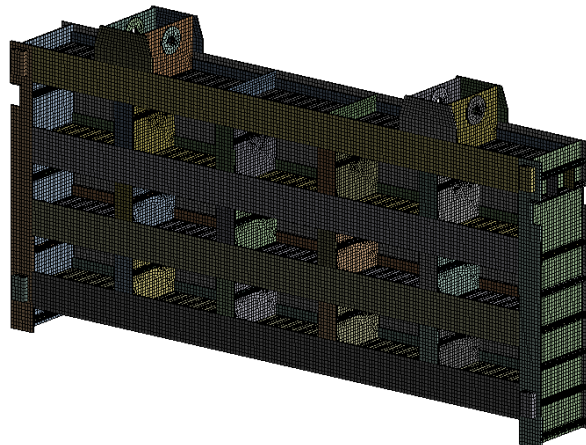


Fig.6 Finite element model of a planar gate

3.2FINITE ELEMENT CALCULATION OF PLANE GATE LOAD

Working condition load considering the gate self-weight, water pressure, the gate installation slider parts to impose lateral displacement constraints on the slider, the water flow direction degrees of freedom and vertical water flow direction degrees of freedom (X, Z direction); the bottom of the gate panel using frictionless constraints (Y direction) in order to simulate the constraints in the vertical direction, and its boundary conditions are shown in Figure 7.

- A: Static Structural**
 Static Structural
 Time: 1. s
- A** Variable Load: Hydrostatic Pressure
 - B** Standard Earth Gravity: 9806.6 mm/s²
 - C** Frictionless Support

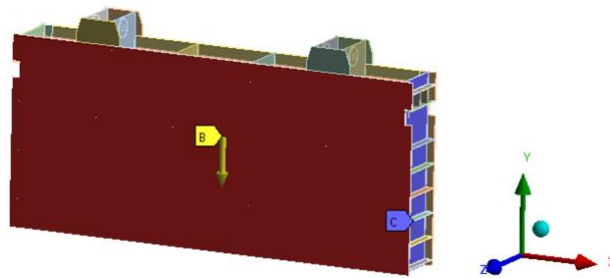


Fig.7 Constraints and loads of the Finite element model

3.3 PLANE GATE SAFETY COEFFICIENT

In this paper, the gate is used for a long time, according to the "water conservancy and hydropower engineering steel gate design specification" [6] (SL74-2019): large and medium-sized projects of the working gate and important accident gate adjustment factor of 0.90 ~ 0.95, medium and large projects of the gate and the starter run 10 years ~ 20 years time factor of 1.00 ~ 0.95, so the time factor is taken as 0.95; the gate is a Deep-water submerged gate, the adjustment factor will be taken as 0.95, so the comprehensive permissible stress adjustment factor is taken as: $0.95 \times 0.95 = 0.9025$

3.4 OVERALL ANALYSIS

The overall structural finite element calculation results of the gate are shown in Figs. 8-16, respectively, and Fig. 9 shows the stress distribution near the overall maximum equivalent force, with the axes orientated in the XY plane.

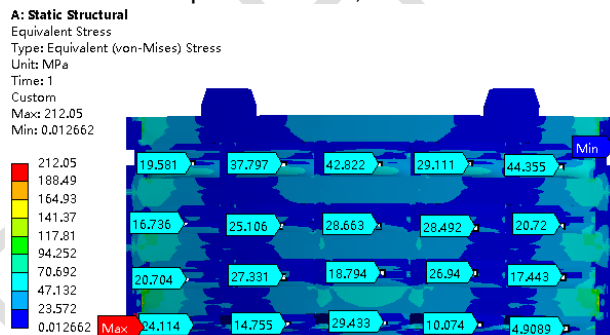


Fig.8 Von-Mises stress contour of the gate

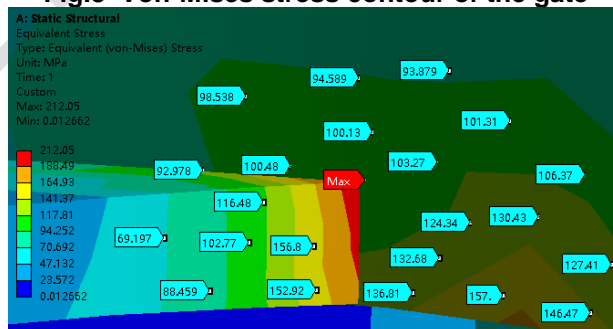


Fig.9 Stress distribution diagram near the overall maximum equivalent stress

A: Static Structural
 Total Deformation
 Type: Total Deformation
 Unit: mm
 Time: 1
 Custom Obsolete
 Max: 4.1567
 Min: 0.0014987

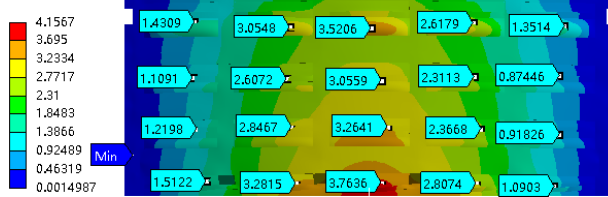


Fig.10 Global displacement contour diagram

A: Static Structural
 Normal Stress 5
 Type: Normal Stress(X Axis)
 Unit: MPa
 Global Coordinate System
 Time: 1
 Max: 155.85
 Min: -197.93



Fig.11 Overall X-axis normal stress

A: Static Structural
 Normal Stress 6
 Type: Normal Stress(Y Axis)
 Unit: MPa
 Global Coordinate System
 Time: 1
 Max: 132.61
 Min: -133.09

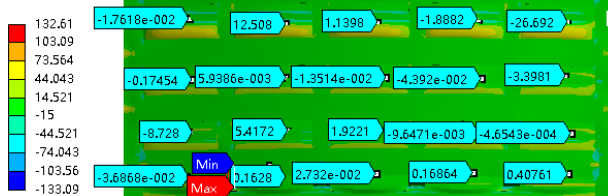


Fig.12 Overall Y-axis normal stress

A: Static Structural
 Normal Stress 7
 Type: Normal Stress(Z Axis)
 Unit: MPa
 Global Coordinate System
 Time: 1
 Max: 134.66
 Min: -177.93

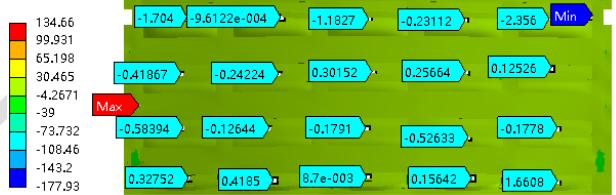


Fig.13 Overall Z-axis normal stress

A: Static Structural
 Shear Stress
 Type: Shear Stress(XY Plane)
 Unit: MPa
 Global Coordinate System
 Time: 1
 Max: 47.299
 Min: -47.298



Fig.14 Overall XY plane shear stress

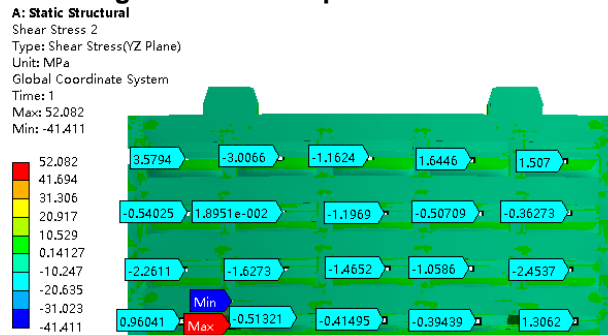


Fig.15 Overall YZ plane shear stress

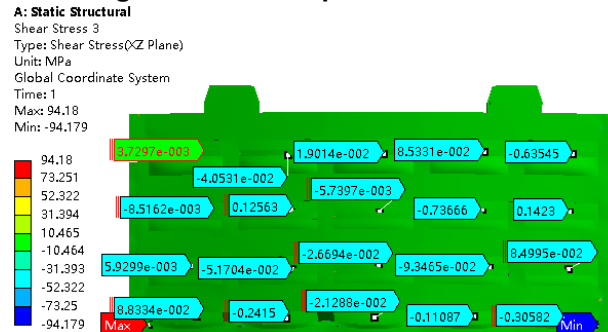


Fig.16 Overall XZ plane shear stress

From Fig. 8 and Fig. 9, it can be seen that the maximum equivalent stress value of the overall structure of the gate is 212.05MPa, which occurs in the connection between the side beams and the main beams, which is less than the permissible yield strength of Q345 311.36MPa, and meets the conditions of use.

Figure 10 shows that the maximum displacement of the overall structure of the gate is 4.16mm, the overall length of the gate is 8640mm, according to the provisions of the maximum deflection of the bending member and the ratio of the calculated span should not be more than 1/750, this paper calculates the ratio of the gate for 1/2077, i.e., 11.52mm, to meet the conditions of use.

From Fig. 11 to Fig. 13, it can be seen that the overall maximum positive stress in three directions of the gate is the vertical water flow direction (X direction) positive stress of -197.93MPa, which occurs in the right side of the lugs and the panel of the connection, and its value is less than the member of the tensile, compressive and flexural permissible stress of 207.58MPa, therefore, the overall structural strength of the gate to meet the specification requirements.

From Fig. 14 to Fig. 16, it can be seen that the overall maximum shear stress of the gate is the horizontal shear stress (XZ plane) of 70.83MPa, which occurs in the connection between the side beams and the lower secondary beams, and its value is less than the allowable shear stress of the member of 121.84MPa, therefore, the overall structural strength of the gate meets the specification requirements.

4.MAIN BEAM ANALYSIS

The main beam section of the gate consists of a web, a front flange and a rear flange, which can be approximated as an I-beam. The next analysis in this paper will use the I-beam model for strength analysis.

In the mechanics of materials, there are two types of beams according to the span-to-height ratio: the slender beam is called slender beam when the span-to-height ratio is greater than 5, and the deep beam is called deep beam when the span-to-height ratio is less than or equal to 5. According to the analysis results for slender beams, the effect of shear force on positive stress is weak, and the positive stress calculation method of pure bending can be used for the analysis of the main beam. However, in fact, the complex structure of the gate, the influence of the constraint mode, load and section shape and other factors, can not just span-height ratio of 5 to define the main beam of the gate. In this paper, the critical span-to-height ratio α_c proposed in Liu Jiliang's "Research on the main frame and dynamic stability analysis method of high head curved steel gates" [8] is used to classify the beam type of rectangular section beams in strength analysis.

The main beam in this paper is a symmetrical I-beam with a length of 8580 mm, and the cross-section dimensions are shown in Fig. 17, where the units are all in millimetres.

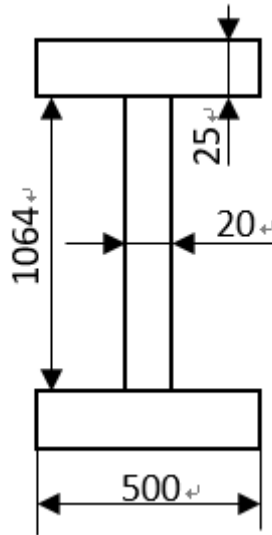


Fig.17 The cross section dimensions of main beam

The maximum positive stress on the cross section of the primary beam in pure bending in mechanics of materials is calculated as equation (1).

$$\sigma_{\max} = \frac{M_{\max} y_{\max}}{I_x} \quad (1)$$

Where, σ_{\max} - maximum bending positive stress;

M_{\max} - maximum bending moment;

y_{\max} - farthest distance from neutral axis;

I_x - moment of inertia.

For I-beams, the maximum bending moment under uniform load occurs in the mid-span section, and the maximum bending moment is calculated as equation (2).

$$M_{\max} = \frac{1}{8} q l^2 \quad (2)$$

The cross-section dimensions are shown in Fig. 18.

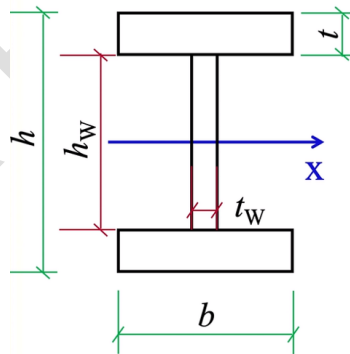
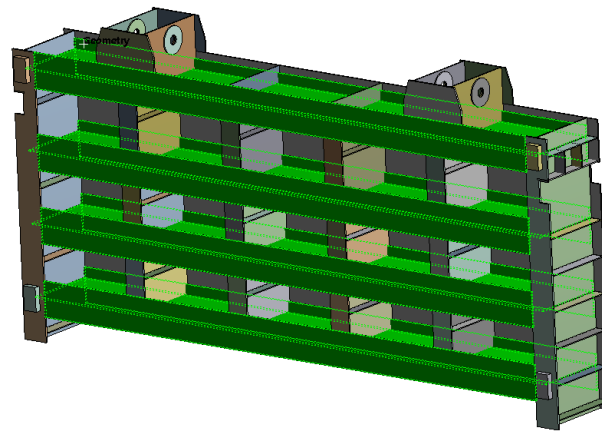


Fig.18 Representation of the cross-sectional dimensions of the main beam

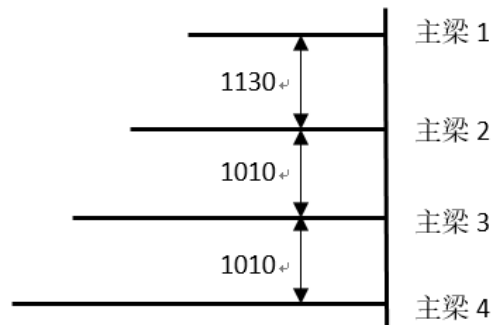
The moment of inertia of the I-beam section on the x-axis is calculated using equation (3), and the meaning of each letter in the equation is shown in Fig. 17.

$$I_x = \frac{t_w h_w^3}{12} + 2 \times \left[\frac{b t^3}{12} + b t \times \left(\frac{h_w + t}{2} \right)^2 \right] \quad (3)$$

According to the drawing data, the total water pressure that the gate is subjected to is 8230 kN. According to the size structure of the main beam of the gate, the main beam of the gate is named from top to bottom from main beam 1 to main beam 4, as shown in Fig. 19(a). The total water pressure is allocated to the main beams according to the geometric dimensions, and the spacing of each main beam and the size of the load to be subjected to homogeneous distribution are shown in Fig. 19 (b), and the figures in the figure are in millimetres.



(a) Gate girder distribution



(b) The value of the spacing of the main beam
Fig.19 Gate girder spacing

The load distribution for each main beam [9] is shown in Table 1.

Table 1 Load distribution table for each main beam

Main beam	1	2	3	4
Water pressure (N)	1.96×10^6	2.03×10^6	2.09×10^6	2.15×10^6

The sum of the water pressures on each main beam should be equal to the total water pressure. According to the water pressure, the uniform load q and the maximum positive bending stress in the span of the main beams can be found, as shown in Tables 2 and 3, respectively.

Table 2 The effective width of the bearing capacity of each main beam and the uniform load value

Main beam	1	2	3	4
Effective width /mm	8580	8580	8580	8580
Distributed load N/mm	228.44	236.60	243.59	250.58

Table 3 Pure bending solution

Main beam	1	2	3	4
Positive stress (MPa)	32.075	36.563	38.467	39.572

The above method is the calculation method of pure bending in the mechanics of materials, but this method simplifies the structure and leads to its calculation error will be relatively large. According to the critical span-to-height ratio α_c equation (4) proposed by Liu Jiliang, in the simply supported beam subjected to uniform load as.

$$\alpha_c = 7.89 \sqrt{2.6(6\beta + 1) + \frac{1.04}{2.6(6\beta + 1)}} \quad (4)$$

According to the calculation of Equation (4) to find that the main beam should belong to the deep beam, rather than the slender beam specified in the mechanics of materials, the shear stress suffered by the non-negligible. Therefore, the bending positive stress calculation needs to consider the effect of warping stress λ , λ calculation formula as equation (5).

$$\lambda = 0.6667 \left[\frac{2.6(6\beta+1)}{\alpha^2} + \frac{0.4}{(6\beta+1)\alpha^2} \right] \quad (5)$$

Therefore, according to the beam bending positive stress calculation formula proposed by Liu Jiliang, the critical span-height ratio αc needs to be considered, and the maximum mid-span bending positive stress in beam bending is expressed by equation (6).

$$\sigma_{\max} = \frac{M_{\max} y_{\max}}{I_x} (1 + \lambda) \quad (6)$$

The results of the calculations are shown in the table below.

Table 4 Deep beam solution

Main beam	1	2	3	4
Positive stress (MPa)	35.924	40.951	43.083	44.321

The finite element method uses discrete units for calculation. By discretising the overall structure of the gate, establishing the connection between the nodes of each unit, setting the external load and boundary conditions, and establishing the linear equations and then solving them. The finite element calculation results will be closer to the actual gate working condition than the theoretical formula calculation results. Using Ansys software to calculate the main beam cross-section of the positive stress, the results are shown in Figure 20 to Figure 23.

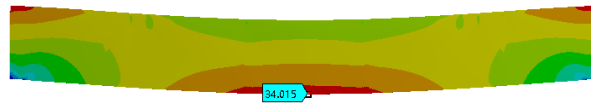


Fig.20 The maximum normal stress of span section of main beam 1

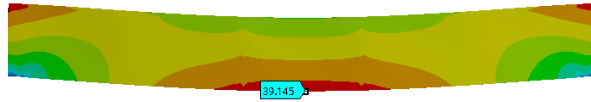


Fig.21 The maximum normal stress of the cross-section of the main beam 2 span

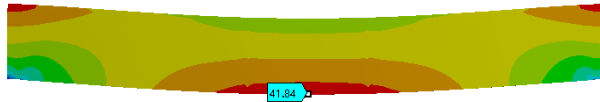


Fig.22 The maximum normal stress of the cross-section of the main beam 3 span

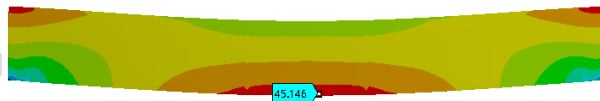


Fig.23 The maximum normal stress of the cross-section of the main beam 4 span

The finite element calculation results are shown in Table 5.

Table 5 Finite element solution

Mainbeam	1	2	3	4
Positive stress (MPa)	34.015	39.145	41.84	45.164

Comparison of the results of the two theoretical calculations with the finite element calculations [10] (in MPa) is shown in Table 6.

Table 6 Comparison of calculation results

Main beam	1	2	3	4
Finite element solution	34.015	39.145	41.84	45.164
Slender Beam	32.075	36.563	38.467	39.572

Solution Error	5.7%	6.6%	8.1%	12.4%
Deep beam solution Error	35.924	40.951	43.083	44.321
Solution Error	5.3%	4.4%	2.9%	1.9%

Table 6 shows that when the main beam is regarded as a deep beam, the error between the calculation results and the finite element solution is small, while when the main beam is regarded as a slender beam, the error between the calculation results and the finite element solution is relatively larger.

The error in the calculation results of the slender beam is large because the force on the main beam is not pure bending but transverse bending, and if the main beam is regarded as a slender beam, the effect of shear will be neglected resulting in inaccurate calculation results. In this paper, the main beam is regarded as a thin-walled deep beam, by establishing a bending-shear coupling mechanical model. The maximum mid-span bending positive stress of the main beam is calculated. The results have relatively small error with the finite element solution, which is more in line with the actual engineering.

5.CONCLUSION

In this paper, the strength of plane gates is analysed. Firstly, the structure and working principle of plane gate are introduced. Using solidworks software to establish the model of the overall gate with reference to the construction drawings, using Ansys software and two theoretical methods to calculate and analyse the structural strength and analysis results.

Firstly, the strength of the gate as a whole was calculated, and it was concluded that its strength was within the standard requirements. Then the main beam of the gate was compared with the detailed calculation and analysis, and the results showed that due to the structural complexity of the gate, the main beam could not be regarded as a simple slender beam for calculation, and the influence of shear stresses needed to be considered, and the calculation was carried out through the establishment of the bending-shear coupling mechanics model. The calculation results show that if the main beam is regarded as a slender beam, the maximum error between the calculation results and the finite element calculation results is 12.4%; while the main beam is regarded as a thin-walled deep beam, the maximum error between the calculation results and the finite element calculation results is 5.3%. Therefore, the strength calculation of the main beam of the gate can not be the main beam as a slender beam, but should be the main beam as a thin-walled deep beam for calculation. The research in this paper provides an important reference for the strength analysis of similar planar gate structures.

REFERENCES

1. Wu Y., Study on flow-excited vibration characteristics of planar steel gates [D]. Zhengzhou University,2021.DOI:10.27466/d.cnki.gzzdu.2021.001772.
2. Chen Yang, Research on vibration characteristics and stability of plane steel gate with fluid-solid coupling [D]. Shandong Agricultural University,2019.
3. Zheng Yajun,Wang Kai,Lei Xingchun,et al. Three-dimensional numerical simulation of pump station inlet flow channel based on RNG turbulence model[J]. Hydropower Energy Science,2008,26(06):123-125. DOI:10.3969/j.issn.1000-7709.2008.06.036.
4. SUN Xiaofeng, MA Yiquan. Research status and development trend of hydraulic gate vibration problem [J]. China Science and Technology Information, 2010, (23): 152-154. DOI: 10.3969/j.issn.1001-8972.2010.23.071.
5. TANG KD, WANG XS, SUN LIUYING. Numerical simulation of flow-solid coupling of arc gate at different openings[J]. People's Yellow River,2019,41(02):135-13. DOI: 10.3969/j.issn.1000-1379.2019.02.029.
6. SL74-2013, Design specification for steel gates for water conservancy and hydropower projects [S]. Beijing: China Water Resources and Hydropower Press, 2013.
7. W. Song. Three-dimensional numerical simulation of upstream and downstream pressurised water flow through gates [D]. Kunming University of Science and Technology, 2020. DOI: CNKI:SUN:ZNSD.0.2019-12-025.
8. Liu Jiliang. Research on the strength and dynamic stability analysis method of the main frame of high head curved steel gate[D]. Northwest Agriculture and Forestry University,2016.
9. Cao Huiying,Ma Renchao,Yu Junyang. Distribution and transfer of water load among the main force components of curved gates[J]. People's Yangtze River,2022,53(01):160-166.DOI:10.16232/j.cnki.1001-4179.2022.01.025.
10. T.Y. Yan,T.C. Li,L.H. Zhao et al. Comparison of finite element methods for solving section internal forces[J]. Hydropower Energy Science,2008(03):141-143. DOI: CNKI:SUN:SDNY.0.2008-03-042.